Investigation of cutting force oscillations when high productivity milling

Dmitry Aleynikov[1], *Anatoly* Lukyanov[1], *Andrey* Savilov[1,*], and *Dmitry* Paikin[1]

[1]Irkutsk National Research Technical University, 664074, Irkutsk, Russia

Abstract. The article analyzes cutting force oscillations of high-productivity milling. Based on end-milling experiments using a milling machine tool, characteristics of spatial oscillations of cutting forces were identified. The data analysis using software and oscillation theory methods showed that at high spindle rotation frequencies under certain milling conditions, interaction of the cutting edges and the workpiece is not uniform which deteriorates the machined surface. As the spindle rotation frequency increases due to resonances in the tool and spindle and mutual oscillations of the workpiece and the tool, the cutting force spectrum varies. Some extra harmonic components appear. They index the failure of interaction of the cutting edges and the workpiece.

1 Introduction

Milling as a technological process is characterized by discontinuous force impacts of the mill on the workpiece [1, 2]. It causes regular cutting force oscillations P(t) with a gear mesh frequency of $f_z=n_1 \cdot z/60=z \cdot f_1$ where n_1 is the angular speed of mill rotation (rpm); z is the number of mill teeth; f_1 is the rotational frequency (Hz). These regular interferences cause forced oscillations of the mill, spindle, tool and workpiece. Mill and workpiece oscillations influence the cutting force. During the high-productivity milling process, resonances and spatial oscillations of the mechanical structure and machine unit occur. They influence the dynamic characteristics of the machine and milling quality [2]. Cutting vibrations also decrease the machine tool resistance. One more negative vibration effect is milling performance degradation due to limited cutting modes.

A set of researches deal with cutting forces during the milling process [3-8]. Their authors develop mathematical models for end milling process simulation. Models describing deformation in cutting found wide application [1, 8, 9, 11]. Along with design and geometry parameters of cutting tools, they take into account material properties. For example, some researchers suggest using cutting force ratios [1, 8, 11]. Orthogonal cutting experiments are carried out to determine their values.

Most researches deal with monolithic end mills made from hard material or high-speed steel [4-7]. A smaller number of works deal with end mills with inserts [8] due to a simpler description of design and geometry parameters of monolithic tools. The fact that the tool body and inserts are made from different materials with different mechanical properties

* Corresponding author: saw@istu.irk.ru

influences the dynamics of cutting. It makes the mathematical process model more complex.

Despite the type of mills, the adequacy of developed mathematical models can be tested. It should be taken into account that in the aircraft industry, high-productivity milling is characterizing by a large volume of chip and is performed with values a_e, which can be equal to the cutting diameter of the tool D_c [7, 8]. Most researchers prefer milling with a small radial cutting depth a_e [9, 10] due to better chip formation control and capacitive constraints, particularly power and a spindle torque. Thus, experimental studies approving the milling process under conditions which are most closely approximate the real manufacturing ones are relevant.

2 Material and method

The experiments were carried out using DMG HSC 75V Linear Milling Machine Center. The machine has a high-speed spindle with a maximum rotation speed of N=28000 rpm. Cutting forces were measured with Kistler 9253B23 which can measure three special force components F_x, F_y, F_z (Fig.1). Technical data of the dynamometer platform are presented in Table 1. Deformable aluminum alloy 1933T2 consisting of Al-89%, Zn-7%, Mg-2%, Cu-1%, Zn-0.15% was used for machining. The samples were 400x300x50 mm in size.

A R790-025HA06S2-16L mill with R790-160408PH-NL H13A inserts was used for milling (Fig. 2).

Fig. 1. The working zone of DMG HSC 75V Linear with Kistler type 9253B23 dynamometer

Fig. 2. R790-025HA06S2-16L mill with R790-160408PH-NL H13A inserts

Table 1. Kistler type 9253B23 dynamometer data

Technical data	**Type**	**9253B23**
Calibrated measuring range		
F_x, F_y	kN	0 … 12
F_z	kN	0 … 25
Natural frequency		
fn(x)	Hz	≈610
fn(y)	Hz	≈570
fn(z)	Hz	≈570
Weight	kg	85

To specify cutting data, modal analysis of the tooling set-up was carried out [1, 11, 12]. Its results and stability lobes are presented in Figure 3.

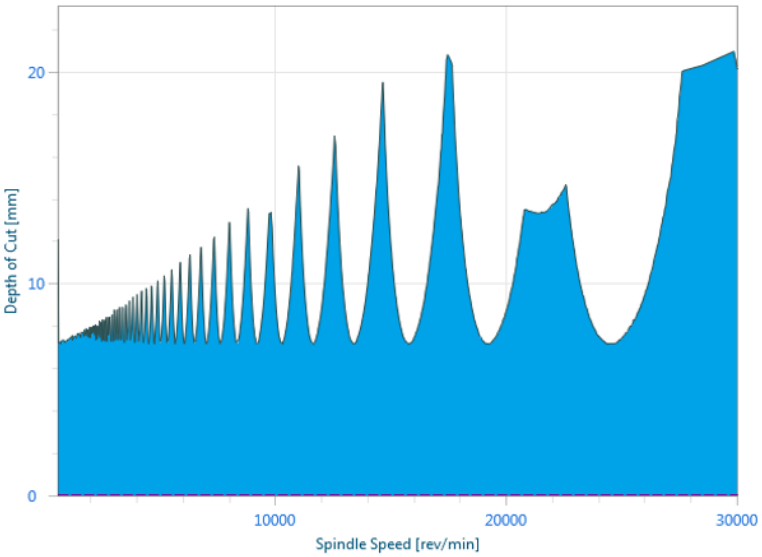

Fig. 3. Stability lobes for R790-025HA06S2-16L mill with R790-160408PH-NL H13A inserts

Based on the modal analysis results, the following cutting data were specified: V_c – cutting speed, a_p – axial cutting depth, a_e – radial cutting depth, f_z – feed per tooth, n_1 – spindle rotation frequency. All these data as well as typical cutting force frequencies and amplitudes on harmonics of rotational Af_1 and gear mesh Af_z frequencies are presented in Table 2.

Table 2. Milling conditions and modal analysis results

No	V_c, m/min	a_p, mm	a_e, mm	f_z, mm/tooth	n_1, rpm	f_1, Hz	Af_1, N	Af_z, N
1	1000	6	10	0,25	12738	212,5	183	222
2	1500	6	10	0,25	19110	318,5	**41**	**198**
3	2000	6	10	0,25	25470	424,5	92	34
4	2150	6	5	0,25	27390	456,5	101	79
5	2150	6	7,5	0,25	27390	456,5	114	90
6	2150	6	10	0,1	27390	456,5	**272**	**18**
7	2150	6	10	0,2	27390	456,5	274	46
8	2150	6	10	0,3	27390	456,5	238	42
9	2150	6	10	0,4	27390	456,5	159	48
10	2150	6	10	0,25	27390	456,5	139	105
11	2150	6	12	0,25	27390	456,5	157	122
12	2150	6	15	0,25	27390	456,5	164	129
13	2150	7	10	0,25	27390	456,5	206	123
14	2150	8	10	0,25	27390	456,5	217	133
15	2150	9	10	0,25	27390	456,5	240	143
16	2150	10	10	0,25	27390	456,5	297	156

3 Results and discussion

Figure 4 shows the oscillograms of three milling force projections F_x, F_y, F_z along feed axis X for measurements 2 and 6. Figure 5 shows milling force oscillation spectra for the same measurements. During the ideal milling process when cutting edges are loaded evenly, the spectral component at a gear mesh frequency f_z exceeds significantly the amplitudes of the other harmonics (see the spectrum in Figure 3 for measurement 2). However, the data of 16 measurements processed in DynoWare developed by Kistler (Fig.4) are opposite. Only for measurements 1 and 2, the amplitudes of spectral components at a gear mesh frequency f_z exceed the amplitude of spectral peaks at rotational frequency f_1. In other measurements, the spectral component of the rotational frequency was fundamental (e.g., see Fig. 5 and 6 of the force spectrum for measurement 6).

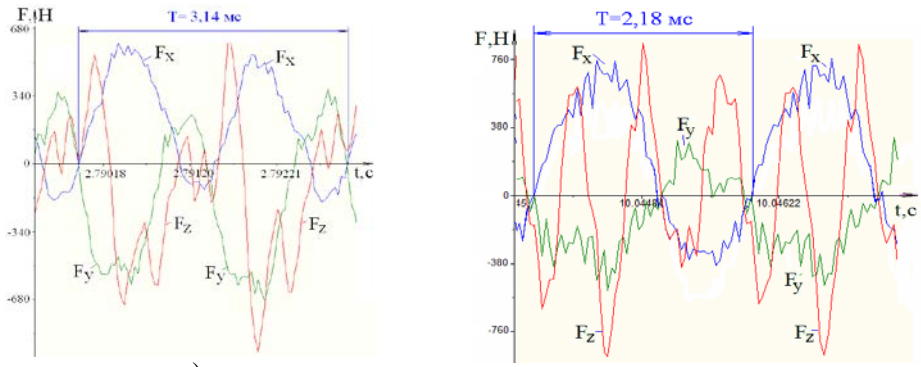

a) b)

Fig. 4. Oscillograms of the milling force along axes F_x, F_y, F_z for measurements 2 (a) and 6 (b).

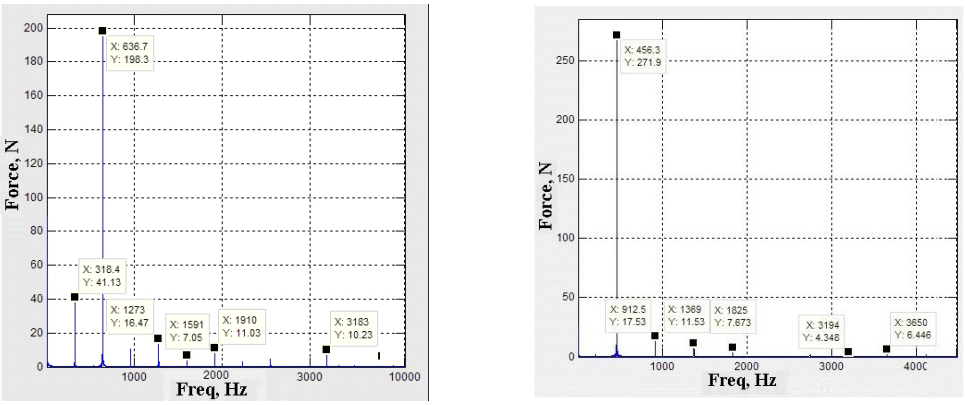

a) b)

Fig. 5. Milling forces vibration spectra along axis X for measurements 2 (a) and 6 (b).

The spectral analysis data for milling forces can be explained from a resonance perspective. In most experiments, natural frequencies of the dynamometer table are close to rotational and gear mesh frequencies of force excitation. Along with its weight, its piezoelectric sensitive elements form a spatial oscillation system which distorts a signal occurring when milling. Therefore, near-resonant oscillations of the Kistler dynamometer platform were calibrated. Figure 6 shows changes in the amplitudes of the first harmonic of rotational and gear mesh frequencies under varying milling conditions.

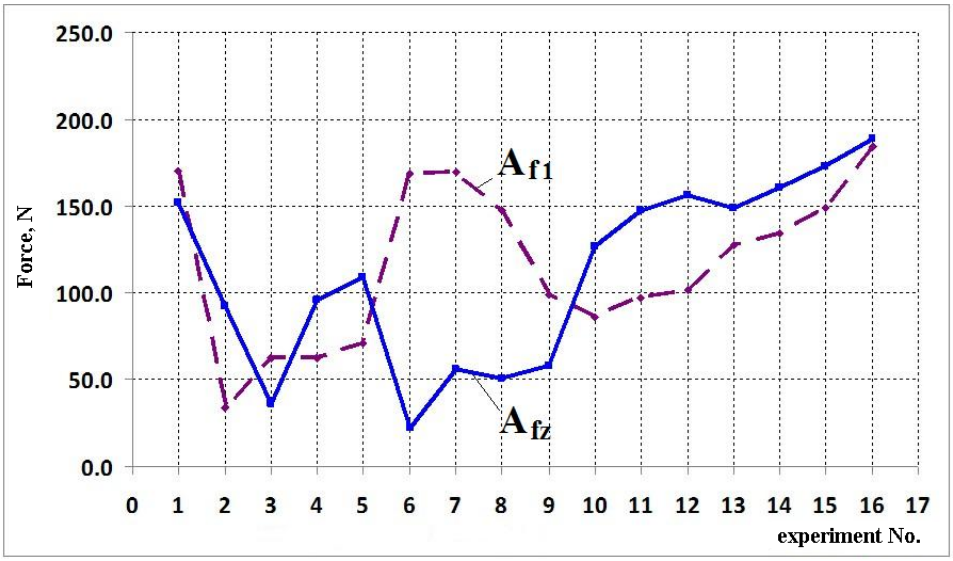

Fig. 6. The curve of varying amplitudes of harmonics of rotational f_1 and gear mesh f_z frequencies after correcting the dynamic error

As can be seen, gear mesh frequency oscillations are not always fundamental. For six measurements (1, 3, 6-9), fundamental oscillations are at a rotational frequency, i.e. at a spindle and mill frequency. For the other measurements, rotational and gear mesh frequency oscillations are comparable.

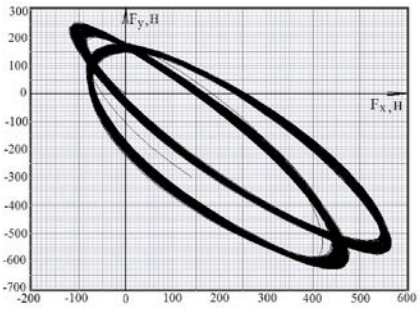

Fig. 7. The orbit of milling forces per 1 sec (318 periods of the rotational frequency) for measurement 2

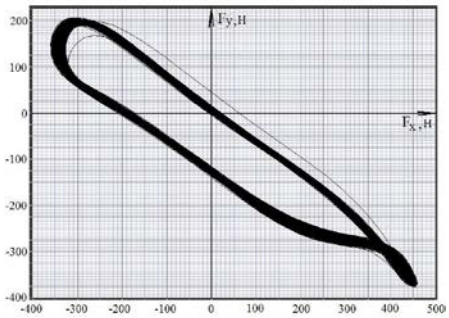

Fig. 8. The orbit of milling forces per 1 sec (458 periods of the rotational frequency) for measurement 6

These conclusions are supported by the diagrams of milling force oscillation orbits in X and Y (Fig. 7,8). For example, for measurement 2 (Fig. 5) when gear mesh frequency oscillations are fundamental, the orbit corresponds to two closed paths. The orbit of milling forces was determined by processing experimental data using LabView and filtering high-frequency harmonics. The orbit of measurement 2 illustrates an ideal milling process when both cutting edges are loaded evenly and work along the chipping area. For measurement 6 (Fig. 8) when rotational frequency oscillations prevail, the orbit of milling forces per 1 sec measurement corresponds to one closed path. The cutting edges work unevenly.

4 Conclusion

As the spindle rotation frequency increases due to resonances of the technological system, the normal conditions of cutting using two edges get disturbed [13-16]. According to the experimental measurements, the frequency of the first mill oscillations was 6820 Hz. Therefore, excitation oscillations with rotational and gear mesh frequencies within the range of 200 Hz to 900 Hz do not influence mill oscillations. Hence, the main factors disturbing the normal milling conditions are resonances of the technological system at high angular spindle rotation speeds.

References

1. Y. Altintas, Manufacturing Automation: Metal Cutting Mechanics, Machine Tool Vibrations, Cambridge: Cambridge University Press, 2012.
2. Lukyanov A.V., Aleynikov D.P., Portnoy A.Y., Bulletin of Irkutsk State Technical University, **21(4)** 30-38 (2017)
3. Kozlov A.M., Kiryuschenko E.V. and Khandozhko A.V., IOP Conference Series: Materials Science and Engineering **177** 012136 (2017)
4. Wen-Hsiang Lai, Tamkang Journal of Science and Engineering, **3** 15-22 (2000)
5. Wu Baohai, Yan Xue, Luo Ming, Gao Ge, Chinese Journal of Aeronautics, **26** 1057-1063 (2013)
6. Takashi Matsumura, Shoichi Tamura, Procedia CIRP **58** 566-571 (2017)
7. Min Wan, Wei-Hong Zhang, Jian-Wei Dang, Yun Yang, Applied Mathematical Modelling **34** 823–836 (2010)
8. Mark A. Rubeo and Tony L. Schmitz, Procedia Manufacturing, **5** 90–105 (2016)
9. U. Karaguzela, M. Bakkal, E. Budak, Procedia CIRP **58** 287–292 (2017)
10. Nikolaev A.Yu., I*OP Conf. Series: Materials Science and Engineering* **177** 012080 (2017)
11. E. Budak and Y. Altintas, Journal of Dynamic Systems, Measurement, and Control, **120**, 10.1115/1.2801317, (1998)
12. Ahmadi K., Altintas Y., Journal of Manufacturing Science and Engineering, 136 (2014)
13. Svinin V.M., Obrabotka metallov/Metall working and material science, **3** 28-30 (2005)
14. B. Balachandran, M.X.Zhao, Meccanica, **35** 89–109 (2000)
15. Campomanes ML, Altintas Y., Journal of Manufacturing Science and Engineering, **125 (3)** 416-422 (2003)
16. Chinesta F., Filice L., Micari F., Rizzuti S. and Umbrello D., International Journal of Material Forming, **1** 507-510 (2008)